Review

Advances in Small Lasers

Martin T. Hill[1], Malte C. Gather[2]

[1] *School of Electrical, Electronic and Computer Engineering, The University of Western Australia, Crawley 6009, Australia, m.t.hill@ieee.org*
[2] *SUPA, School of Physics and Astronomy, University of St Andrews, North Haugh, St Andrews KY16 9SS, UK, mcg6@st-andrews.ac.uk*

Abstract

In recent years there have been significant advances in the size and characteristics of small lasers, i.e. lasers with dimensions or modes sizes close to or smaller than the wavelength of emitted light. This work has primarily been led by innovative use of new materials and cavity designs. This article reviews some of the latest developments, particularly in metallic and plasmonic lasers, improvements in small dielectric lasers, and the emerging area of small bio-compatible/bio-derived lasers. We examine the different approaches employed in small lasers to reduce size and how they lead to significant differences , particularly between metal and dielectric cavity lasers. We present potential applications for the various forms of small lasers and indicate where further developments are required.

Introduction

Miniaturization and integration of photonic components has led to improved systems and opened up new application areas, somewhat in analogy to the development in electronics. Lasers are an area of photonics where miniaturization holds particular promise but also one where miniaturization has turned out to be particularly challenging. Potential applications of ever smaller lasers include on-chip optical communication and data processing which may allow data rates beyond what is feasible in the realm of electronics[1–3]. Continued miniaturization of lasers may also open new avenues in medical imaging and sensing if such lasers can be made biocompatible and implantable[4,5]. Likewise, 3D displays and advanced holography may benefit from considerably more compact coherent light sources[6].

The invention of the VCSEL (vertical cavity surface emitting laser) in the 1980's and early 1990's[7,8] heralded the first miniaturized lasers with dimensions on the order of several wavelengths of the emitted light. In the 1990's further steps in miniaturization were taken with the demonstration of microdisk lasers[9], photonic crystal lasers[10] and lasers consisting of self-assembled nanowires[11]. While most of this pioneering work relied on conventional semiconductors and patterning by top-down lithography, the use of new gain materials, such as organic semiconductors[12] and nanocrystal quantum dots[13], enabled more bottom-up type fabrication methods for lasers and provided additional flexibility, e.g. with respect to cavity design and emission wavelength. All of these lasers use differences in the refractive index of dielectrics to confine the light in the cavity, resulting in the overall size of the laser to be larger than the wavelength of the emitted light, and the minimum possible optical mode size being determined by the diffraction limit. More recently, metal based resonant cavity structures have enabled shrinking both the overall size of the laser to less than the wavelength of light, and the dimensions of the optical mode to less than the diffraction limit[14–20].

The progress in laser miniaturization over the last few decades is summarized in Fig. 1, giving examples of several small lasers, with the images scaled in size to their lasing wavelength. It appears to take 10 to 20 years from initial proof of concept of lasing, often done at low temperature, until devices useful for applications are obtained (Fig. 1). The latter typically requires CW (continuous wave) operation at room temperature (RT), ideally with direct electrical pumping, a reasonable lifetime, and certain characteristics that established types of lasers cannot offer.

In this article we review the recent progress towards ever more compact lasers. Each type of laser uses a particular strategy to address the fundamental challenges involved in making a smaller laser. The key laser characteristics that result from each strategy are examined and applications benefitting from them are identified. Remaining challenges for further miniaturization and obtaining devices useful for applications are discussed.

Limits on laser size

A simplified laser model is examined to better understand ultimate limits on laser size, which features of each type of small laser are exploited to obtain miniaturization, and how these features impact on device characteristics and ultimate miniaturization limits. Figure 2 shows conceptually a generalized laser resonator (in this case a Fabry-Perot cavity) of length L, with end mirror reflectivities R_1 and R_2, resonant at free space wavelength λ_0, propagating a mode with effective index n and propagation loss α_i along the central waveguide. (Note that the effective index n can differ significantly from the index of the waveguide core, especially in the plasmonic structures discussed below.) Lasing sets in when the electric field amplitude at an arbitrary point in the cavity E_0 returns to its original value after the light makes a round trip through the resonator, i.e.:

$$E_0\sqrt{R_1R_2}e^{(G_m-\alpha_i)L}e^{i2nL/\lambda_0} = E_0 \qquad (1)$$

Here, G_m is the modal optical gain (see below). The complex exponential in Eq. (1) needs to be a multiple of 2π which leads to the cavity length requirement

$$L = \frac{\lambda_0}{2n}m \qquad (2)$$

where m is an integer. The shortest possible cavity length is thus half a wavelength (m=1).

The amplitude component of Eq. (1) leads to another requirement on the cavity length L; that is the modal gain G_m must overcome the internal absorption loss α_i and the mirror losses in one round trip:

$$L = \frac{-\ln(R_1R_2)}{2(G_m-\alpha_i)} \qquad (3)$$

G_m is typically related to the material gain G_a of the active region material by the confinement factor Γ which describes the fractional overlap of the laser mode volume V_0 with the volume of the active region V_a:

$$G_m = \Gamma G_a \qquad (4)$$

In the absence of optical gain and lasing, the lifetime of a photon in the cavity τ_p is given by the cavity parameters introduced above or by the more generally applicable quality factor of the cavity Q:

$$\frac{1}{\tau_p} = c\,\frac{\alpha_i + (1/(2L))\ln(R_1R_2)}{n} = \frac{2\pi c}{Q\lambda_0} \qquad (5)$$

At laser threshold the modal gain is therefore related to photon lifetime by:

$$\frac{1}{\tau_p} \sim c\Gamma G_a/n \qquad (6)$$

We have assumed that the phase and group velocity of light in the cavity are the same, also that Γ can be calculated from the overlap of the modal electric field energy with the gain medium, which is in general not true[21,22]. When Γ is taken as waveguide confinement, it can be greater than one[21,22], making modal gain higher than material gain, though material gain required for threshold may not be reduced due to increased group index[21] n. However, when Γ is taken as an energy confinement factor, it is always less than one[21]. The smallest lasers may not be based on a propagating mode, but one can still assign an energy confinement factor Γ and a photon (or plasmon) lifetime, so many of the key parameters and concepts of the various classes of small lasers can be compared and explained via the simplified model.

How do lasers become compatible with electronic device dimensions which are on the order of tens or hundreds of nanometers? Considering first laser length, the lower limit to L is determined by the phase limit (Eq. 2) and the modal gain limit (Eq. 4). Due to their high refractive index, semiconductors allow lasers with a phase limit on L on the order of a few hundred nanometers. As discussed later, this can be reduced further by increasing n. In practice, the gain limit is often the greater constraint on L, as the cavity needs to be long enough to compensate for the mirror losses. To reduce the gain size constraint, mirror losses need to be reduced, Q factor increased, and modal gain needs to be increased by increasing Γ and G_a.

There are also fundamental restrictions on the transverse dimension of lasers. For lasers based on dielectric waveguides, reducing the thickness d of the waveguide formed by the central active material much below the wavelength of the bulk wave in the medium leads to substantial broadening of the transverse field[14] (Fig. 2b,c). By contrast, metallic or plasmonic waveguides such as metal insulator metal (MIM)[16] structures allow reduced transverse dimensions and a sub-wavelength localized transverse field albeit at the cost of increased α_i due to absorption in the metal[14,16] (Fig. 2c). Generally, reducing transverse laser dimensions involves complex tradeoffs between Γ, V_a and α_i as will be discussed later.

Shrinking the dimensions of electronic devices often yields improved characteristics, in particular higher speed. The modulation bandwidth of a laser, which is determined by the delay incurred between turning the laser off and the end of laser emission, is ultimately limited by the photon lifetime τ_p. Particularly for direct electrical modulation, which will be important for communication applications, factors like non-linear gain compression restrict the modulation bandwidth before the τ_p limit is reached[23]. Small laser cavities have also been shown to significantly modify the rate of spontaneous emission[17,19,20] which can enhance the modulation bandwidth, particularly if the cavity is used as a light emitting diode rather than a laser[23–26]. In optical signal processing applications however, optical modulation bandwidth could approach the photon lifetime limit[27]. Achieving shorter τ_p requires increased internal and mirror losses and thus again demands higher G_m (via improved Γ and G_a).

Considering other desirable laser characteristics: Low power operation generally requires a large τ_p and a high Γ in order to keep the material gain required to reach the lasing threshold low. Combined with a small active medium volume and a range of other technical factors, this will minimize the absolute pump energy required to reach threshold. At the same time the total output power of lasers with small active medium and large τ_p is naturally less than for many conventional lasers. However, as discussed later, for many applications it is more relevant to achieve low power operation, i.e. obtain low threshold and high conversion efficiency between pump and laser output (slope efficiency). Balancing threshold and slope efficiency often involves a tradeoff between internal losses and mirror losses. Spectral purity may also be a priority for certain applications, in which case a higher Q is desirable as laser linewidth is inversely proportional to Q[26].

Active materials for small lasers

In comparison to macroscopic lasers, small lasers require active materials with large material gain G_a as mirror losses have to be compensated over a shorter length and as internal losses are often higher. This limits the choice of active materials to

liquid and solid-state gain media. Fig. 3a compares optical gains achieved in different families of gain materials with relevance to small lasers.

Inorganic solid-state materials, in particular semiconductors, are the most widely used gain material. They allow direct electrical pumping and provide high optical gain from a few hundred per cm for bulk semiconductors[21] to > 5×10^4 cm^{-1} in quantum dot structures[28]. Even higher optical gain, up to many thousands per cm for bulk semiconductors, has been inferred from recent experiments on metallic lasers and nanowire lasers[17,18,20,29,30]. Although these numbers have not been confirmed via direct amplification measurements, they are consistent with predictions of theoretical models for high carrier densities[21] and the low group velocity of light in small plasmonic waveguide lasers[18,20]. Particularly high gain has mostly been found for devices operated at low temperatures, however, even for room temperature electrically pumped lasers bulk material gain of ~940 cm^{-1} is inferred, albeit with a limited device lifetime due to the high injection currents [31]. High current injection can cause significant device heating and limit gain. However, experiments with surface emitting metallic lasers have inferred quantum well gains of over 8400 cm^{-1}, even at room temperature with continuous electrical pumping[32]. For quantum dot and quantum well structures the available modal gain is often significantly lower than the material gain due to the limited overlap of the mode with the small quantum dots. Nevertheless, carefully designed structures, such as high density quantum dots[23] or strained quantum well super-lattices[27], may provide advantages over bulk semiconductors for small metal lasers.

Tuning the emission wavelength of conventional semiconductors and integrating them with other materials (e.g. metallic nanostructures) usually requires complex deposition and lithography processes. Alternative material classes that offer a more bottom-up device fabrication include organic dyes, organic semiconductors and colloidal quantum dot nanocrystals. These materials can be readily prepared as thin films (e.g., with thicknesses << 1 μm) by solution-based processes. In some cases, structures providing optical feedback can even form via self-assembly[33–35]. Moreover, the gain spectrum of these materials can be readily tuned by targeted modifications of chemical structure, composition and characteristic dimension (Fig. 3b). Additionally, the gain spectrum is typically rather broad so that the laser wavelength can be tuned over considerable ranges without exchanging the material[36].

Organic dyes solutions have historically been used in macroscopic, wavelength tunable dye-lasers operating at visible and near-infrared wavelengths. Recently, microfluidics enabled their application in small lasers[37–40]. A particular advantage of these fluidic lasers is that refractive index and gain spectrum of the active medium are tunable by exchanging the solvent or the dye passed through the device. Alternatively, organic dyes can be embedded in a transparent and mechanically flexible solid-state matrix, often an organic polymer[41,42]. Like organic dyes, organic semiconductors[12] are hydrocarbon based compounds with strong optical transitions. In addition, their large conjugated π-electron systems confer semiconducting properties, opening up the prospect of direct current injection although the low charge carrier mobility of organic semiconductors has so far prevented lasing through direct electrical pumping in these materials. Strategies to obtain materials with improved charge mobility and high optical gain involve fine-tuning the conjugated backbone of polymeric materials or introducing long-range order[43,44]. Optically pumped organic semiconductor laser configurations have been explored in considerable detail. Besides representing an intermediate step towards electrically pumped organic lasers, these devices also find direct applications, e.g. when coupled with inexpensive LED pump sources[45].

Under high excitation conditions, organic materials can show photo-induced bleaching of fluorescence and optical gain which is a concern when long-term operational stability is required at high power densities. Inorganic colloidal quantum dots retain many of the attractive properties of organic materials –such as solution-based processibility and good tunability of the emission (Fig. 3b) [46]– while at the same time potentially offering better stability. Compared to epitaxially grown quantum dots, they are typically smaller (radius, approx. 1 - 4 nm) and frequently use core-shell structures with CdSe, CdTe,

or PbS cores and ZnS or CdZnS shells. Under sub-picosecond optical excitation, the optical gain in thin films of quantum dots can be up to hundreds per cm and lasing has been demonstrated with different laser configurations and across a wide range of wavelengths[13,47].

Small laser types and their characteristics.

Figure 3c,d,e summarizes a number of key laser parameters for various literature examples of different laser types: Firstly, a key minimum dimension of the laser is listed, for example, the length of the VCSEL cavity, the size of Bragg gratings, or disk size, indicating some limit to how small the laser can be. Secondly, the overall volume taken up by the laser is given. To allow a fair comparison, both parameters are normalized to the free space wavelength at which the laser emits. The *Q* factor and the lasing threshold are also listed for the different examples as an indication of performance. It can be seen that with respect to laser size and *Q* factor, there is a clear divide between metallic and dielectric cavity lasers.

VCSELs solve the problem of making a small laser by having very high reflectivity Bragg mirrors ($R_{1,2}$~0.99) and low internal losses so that only a small amount of gain material is required in the center of the laser. The high reflectivity mirrors lead to a high *Q* and long photon lifetime on the order of picoseconds (Fig. 3d). However, the Bragg mirrors result in an overall device thickness on the order of several microns (Fig. 3c). The transverse size is often several wavelengths to limit surface roughness induced internal losses and to maintain high Γ. It took over a decade from the initial demonstration of the VCSEL[7] at low temperatures until CW electrically pumped room temperature devices were created[8], a process that involved significant manufacturing improvements (e.g., monolithic growth of active material and Bragg mirrors). However, once this milestone had been reached, the development became very rapid and useful commercial devices appeared by the late 1990s[48]. Due to the long photon lifetime and small V_a, small threshold currents –on the order of 10 μA– have been reported[49]. VCSELs have also been realized with organic semiconductors[12,50], colloidal quantum dots[47] and bacteria biofilms that produce a fluorescent protein[51]. Furthermore, the VCSEL geometry is frequently used to study exciton-polariton condensation (see Box: Exciton-Polariton Lasers).

Small nanowire lasers are conceptually similar to VCSELs in that feedback is provided by short (few μm) Fabry-Perot type resonators. However, their transverse size is often much smaller, a few hundred nanometers or less. These cavities can have *R* reaching ~0.9, not as high as VCSELs, so that a gain medium that occupies most of the cavity and thus gives a large Γ is required for lasing[22]. Small nanowire lasers have only been demonstrated under strong optical pumping with recent examples exhibiting complex nanowire growth[29,30]. Self-assembled organic semiconductor nanowires have also yielded small lasers (300 nm diameter, 6 μm length) without the need for lithographic patterning[33]. In a similar fashion, internal reflection in micro-crystals of organic semiconductors has been used to define Fabry-Perot type cavities[35].

Microdisk lasers consist of a thin disk of semiconductor in which whispering gallery modes circulate around the edge of the disk. For disks of sufficient size, the quality factor of particular whispering gallery modes can be high (typically on the order of 10^3, but up to 10^7 has been demonstrated)[52], leading to photon lifetimes of several picoseconds. Again the approach of a long photon lifetime (equivalent to high *R* in the model introduced earlier) allows reduction of the size of the laser. The smallest CW electrically pumped devices have cavity sizes on the order of 3 μm in the transverse direction[53]. The device thickness can be on the order of several hundred nanometers, although the pillars needed for electrical pumping increase device height. Optically pumped devices can be even smaller, with disk diameters down to the sub-micron level[54] even though decreasing diameter generally increases radiative losses and reduces Γ. The initial demonstrations of microdisk lasers occurred in the early 1990's[9]. Improved fabrication techniques led to CW electrical pumping in the late 1990's, and in the late 2000's the first experimental applications in on chip communications were shown[55]. Again, due to the small V_a and

long photon lifetimes, reasonably small threshold currents (< 100 μA) have been achieved[53]. The highest *Q* factors are typically achieved in SiO_2 based toroid structures fabricated by a melt-flow process[52]. Under optical pumping one can also use three dimensional (3D) microsphere geometries instead of the two dimensional (2D) microdisk configuration. Spherical microcavity lasers have been realized based on Raman gain in silica[56], dye doped microspheres[42], or microdroplets of liquid gain material[38]. For the latter, microdroplet size and composition can be adjusted with microfluidics to tune laser characteristics.

Photonic Crystal Lasers were first demonstrated in 1998[10]. These structures use 2D or 3D Bragg gratings to confine light to diffraction limited volumes, with 2D grating devices having confinement in the third dimension via total internal reflection. The structures typically have dimensions on the order of several μm in the transverse direction, in order to accommodate the several Bragg layers needed to make high reflectivity mirrors whereas the thickness is typically several hundred nanometers. Initial devices operating at low temperature and under pulsed optical pumping had low *Q*s on the order of several hundred. However, over the last decade improved technology led to greatly improved *Q* factors for photonic crystal cavities. The first devices to show either room temperature optically pumped operation or pulsed electrical pumping had *Q*s on the order of 3,000[57]. More recently, 3D photonic crystal structures with complete bandgap reached *Q* factors on the order of 40,000[58]. The suspended membrane structure of many photonic crystal laser designs leads to poor heat-sinking of the active region and renders it difficult to add electrical contacts. Hence, it has not been until recently that CW room temperature electrical pumped operation has been achieved in these lasers[59]. The much smaller active region in these latest devices has led to the lowest threshold currents for any CW semiconductor laser operating at room temperature.

In the realm of organic materials, lasers based on one dimensional (1D) Bragg gratings are highly popular, and pulsed optically pumped lasing is obtained with thresholds < 50 pJ [60] and < 1kW/cm^{-2} [45]. Distributed feedback (DFB) structures can be written into these gain materials directly using electron-beam or interference lithography; for certain materials even in a rewritable fashion, hence allowing a post-fabrication adjustment of the resonant wavelength[41,61]. Organic lasers based on 2D photonic crystal structures[62] and small dye lasers comprising of 3D inverse opal structures[34] have also been demonstrated. Microfluidic lasers also benefit from photonic crystals; circular gratings and photonic band-gap fibers have been used to reduce laser footprint[37,39].

Non-Plasmon Mode Small Metallic Lasers. The first small metal cavity lasers employed TE (transverse electric) or HE (hybrid electric) modes of the metallic structures, which had a non-plasmon or non-evanescent transverse field. The miniaturization of such devices is limited to the diffraction limit; one of the smallest devices of this kind was reported in 2007 and has a transverse size of ~260 nm (Fig. 4a)[17]. A popular structure comprises of a metal encapsulated high gain material[17,63]. However, several other forms have been demonstrated, such as nanopatch devices[64], with a size of just 500 nm in their largest dimension, or vertical travelling-wave core-shell structures terminated by Bragg gratings[65]. The non-plasmon mode metallic lasers often have *Q* factors as low as 100 - 200, but can have *Q*s of several thousand[63] depending on the structure and nature of the mode. The strategy of these lasers is quite different from small dielectric lasers in that one enhances confinement Γ and obtains very small V_a through a metal cladding. This limits transverse size, however at the cost of high internal losses due to absorption by the metal. Depending on the design, very high pump densities may therefore be required and lasing may only be achieved close to the maximum gain available from the employed material. However, the metallic structures provide good heat-sinking[65] and readily enable electrical contacting. In addition, the small V_a should in theory result in small absolute threshold currents. It took less than six years from the first demonstration of this form of laser until CW lasing was achieved at room temperature and under electrical pumping[31].

Plasmon Mode Small Metallic Lasers. These are metallic devices based on surface plasmon polariton (SPP) modes. SPP are modes confined to the interface of a dielectric and a conductor and decay exponentially away from the interface. So far,

most demonstrations have exploited propagating SPP modes which are far from the metal resonance, allowing confinement over a broad range of wavelengths, with the propagation wavelength not differing dramatically from that of light in the dielectric[15]. Propagating SPP modes can occur at single metal dielectric interfaces, such as metal surfaces loaded with a gain material[20,25], or at dual interface metal-insulator-metal (MIM)[16,18] and insulator-metal-insulator (IMI)[16] waveguide structures. IMI structures can support long range SPPs[66] and compensation of propagation loss in IMI waveguides embedded in organic gain materials has been studied using optical amplifier configurations without optical feedback[67,68]. The first small plasmon mode lasers demonstrated in 2009 operated at low temperature, and consisted of Fabry-Perot cavities formed from sections of either MIM or gain loaded plasmon mode waveguide (Fig. 4b)[18,20]. Further forms of small cavities such as plasmonic photonic crystal cavities (Fig. 4c)[69] or whispering gallery mode cavities (Fig. 4d)[70,71] can be obtained by patterning either the dielectric near the metal interface or the metal itself. For plasmon mode cavities, the electromagnetic field in the transverse direction is evanescent and so the transverse dimensions of the optical mode and device can be much smaller than $\lambda_0/2n$. (Fig. 2b illustrates this schematically for a MIM waveguide supporting a plasmon gap mode, i.e. a mode where the electromagnetic field is 'squeezed' into the dielectric gap between two metal layers and is the lowest order symmetric transverse magnetic mode.) The length limit of $\lambda_0/2n$ still applies in the propagation direction. However, the actual value can also be smaller than in dielectric structures because the effective index of the plasmon mode may be higher than the effective index of the modes in a dielectric waveguide. To illustrate the tradeoffs involved in reducing transverse dimensions with plasmon modes, we consider 1D confinement in a MIM waveguide supporting a plasmon gap mode. Silver is used as metal, the insulator bulk index is 3.6 and the thickness *d* is $0.05\lambda_0$ with λ_0 = 1.55 μm as vacuum wavelength. From Fig. 2c it can be seen that the spatial extent[16] of the *H* field is 117 nm, significantly smaller than for a dielectric waveguide of the same dimensions (346 nm). However, a propagation loss of 1012 cm^{-1} is incurred in this structure, which yields a maximum *Q* of 192 (assuming *R* = 1, group index = 4.8). Smaller transverse dimensions will give greater propagation loss and hence lower Q. In practice, surface roughness induced scattering leads to further increases in loss and optimizing roughness helps to manage losses to some extent[72,73]. Even though Γ is relatively high for plasmon mode lasers, high losses often lead to extreme pumping requirements. Initial work was often based on optical pumping and/or required low temperatures, though there has been rapid improvement[18,74,75]. Again, the proximity of metals to the gain medium and the optical mode help to dissipate heat originating from high injection currents and high optical intensity. We performed simple thermal modelling of a photonic crystal semiconductor-air membrane laser[59]and a MIM structure with the semiconductor enclosed in silver (using CoventorWare software). We find that the thermal resistance from a small active region to a heat sink can be one to two orders of magnitude less for the MIM structure. In the future, this important thermal advantage of metal devices should be confirmed by more detailed investigations.

Metallic nano-particles are another form of resonator which uses localized non-propagating plasmon modes[19,76]. Here, the metallic nano-particle dimensions are much smaller than the wavelength of the light and the interaction of the particle with light can therefore be described by a quasi-static approximation[76]. If sufficient optical gain is provided by the media surrounding the nano-particle or localized surface plasmon, stimulated emission of surface plasmons is expected. Localized surface plasmon devices in which the gain overcomes the system losses are often referred to as *SPASER*s (surface plasmon amplification and stimulated emission of radiation)[76]. However, in the literature this term has also been used for other plasmon based lasers. To our knowledge, there have been only few demonstrations of such localized plasmon lasers until now[19,77]. These *SPASER*s were based either on dye coated Au nanoparticles (Fig. 1e) or on Au nanorods embedded in a dye loaded polymer matrix. The experiments looked at a large ensemble of many of these devices (>10^6). An experimental demonstration of a single isolated device has yet to be shown. Other studies of similar configurations have found evidence of strong coupling of the gain material to the plasmon mode (evidenced by considerable reductions in excited state lifetime) but have not observed spaser action[78]. The metal losses in these localized surface plasmon cavities are very high, with *Q* factors of just a few tens, hence the material gain required to overcome losses is predicted to be on the order of 10^5 cm^{-1} [79].

It has been noted that it may be difficult to observe a clear threshold in SPASER cavities as the very high Purcell effect reduces the spontaneous emission lifetime of the gain medium[80]. Furthermore for electrically pumped truly sub-wavelength *SPASER*s, current densities will have to approach MA/cm^2, making their practicality dubious[80]. Alternatively, arrays of strongly coupled plasmonic nanocavities can harness some of the advantages of localized surface plasmons, like the dramatically increased spontaneous emission rates, while at the same time reducing the gain required to reach the lasing threshold to a regime that is compatible with the gain available from organic dyes[81,82]. Similar resonant effects were also observed in random ensembles of metallic nanoparticles coated with optical gain media[83]. However, the overall dimensions of such lasers are obviously orders of magnitude larger than the single nanoparticles or nanocavities they are based on.

Applications

The use of small lasers for short distance communications between or even within integrated circuits attracts significant interest. The target energy for the laser transmitter in this context is 10 fJ per bit[1]. Photonic crystal lasers appear to offer an acceptable solution for this application, as they have moderate active region volumes, provide high *Q* thus permitting low threshold currents, can be coupled directly to waveguides, and will likely offer a reasonable modulation bandwidth at least into the tens of GHz. Recent electrically pumped photonic crystal lasers have indeed exceeded the 10 fJ energy target[59]. Metallic nano-cavity devices are another promising candidate[84] as they can have much smaller active regions than dielectric cavity lasers. Although their low Q factors typically lead to higher threshold currents, some design studies predict that metallic structures coupled to waveguides could offer very small footprint devices with sufficient efficiency for this application (Fig. 5a)[84]. Furthermore, it is predicted that due to their sub-wavelength sized, low *Q* factor cavities, metallic devices can provide the highest possible modulation bandwidth[23].

Digital optical information processing is another area where small lasers may find applications[2]. Due to their small size and low Q, small plasmonic lasers are predicted to have intrinsic bandwidths in the region of at least 1 THz[24,25] while requiring moderate power, thus offering potential advantages over high speed electronics. However, even if such lasers become available, issues such as directional flow of information, isolation between inputs and outputs of digital devices, and robustness of the devices to operating and manufacturing tolerances need to be addressed. Recent waveguide embedded nanolasers show that over time such problems might be solved[85]. A related application with less stringent requirements is the use of other small plasmonic devices such as detectors, waveguides and modulators for an integrated optics platform with increased performance, and greatly reduced size and power consumption[3]. Efficient sub-wavelength plasmonic amplifiers and lasers are a prerequisite for any complex plasmonic integrated circuit as absorption by the metal needs to be compensated for in these circuits (Fig. 5b)[67,68].

Small low-power, efficient laser sources are also useful for sensing applications, particularly when coupled with integrated optical cavities. Plasmonic resonators provide a broad bandwidth with strong spontaneous emission enhancement due to the small cavity volume whereas dielectric resonators tend to be larger but offer narrower bandwidth. Small lasers have also been used as sensors directly. The high sensitivity of microdisk lasers to changes in the ambient refractive index, for example, has enabled the detection of single virus particles attaching to the surface of an Er-doped silica microdisk laser (Fig. 5c)[86]. Another study found that protein adsorption kinetics can be measured with improved signal-to-noise ratio when using whispering gallery mode resonators based on fluorescent polymer microspheres and operating these above the laser threshold[87]. For biosensing, lasers based on biologically produced materials, such as green fluorescent protein[4,51] or fluorescent vitamins[88] are uniquely suited to generate laser light within living organisms (Fig. 5d). Using the small laser configurations discussed above, intracellular lasing could be achieved without an external resonator, which may enable

novel nonlinear imaging schemes or dense wavelength multiplexing. Micro-lasers based on fluorescently labeled DNA as gain medium may find applications in optical DNA sequencing[89].

Future trends and challenges

After many attempts by a number of groups[57,90,91], recent work employing improved heat-sinking has shown that photonic crystal lasers are suitable for electrically pumped applications even though complex active/passive re-growth technology capable of forming wavelength scale features was required[59]. However, one can expect that established concepts for passive photonic crystals, e.g. for cavities and waveguides, can be applied to photonic crystal lasers.

Like small dielectric lasers, the more recently developed small metallic and plasmonic lasers can be realized with a widely varying range of laser resonator structures, from plasmonic photonic crystal structures and open dielectric-loaded waveguides[20,69–71,74,81,92,93] to small encapsulated devices or metallic nano-particle resonators[17–19,63–65]. There is potential for further development of different forms of metallic waveguides, permitting possibly better tradeoffs between small volume and metal induced losses. More advanced gain materials, such as strained quantum wells, may also provide significantly improved performance, compared to the bulk material used in most initial experiments.

A key issue to be solved for both photonic crystal and metallic nano-lasers will be device lifetime. The small gain regions in these devices have large surface to volume ratios and their fabrication often involves etching which can introduce surface defects and surface recombination that accelerate device aging.

For the smallest nano-laser, the SPASER, which is much smaller than the wavelength of light in all dimensions, demonstrations have been given of resonance narrowing in samples containing multiple small resonators. However, spasing from a single localized resonator has not been shown, yet. In principle, the output of individual resonators could be probed by either scanning near field microscopy (SNOM) or by creating well-separated individual resonators (via lithography). Individual lasers with deep sub wavelength confinement of mode and gain medium have yet to be shown, even with just one dimensional confinement.

Some applications may already benefit from the advantages that metallic/plasmonic lasers offer, in particular their extremely localized and high intensity fields. However, for more conventional applications such as communications, computing and light sources, metallic nanolasers require substantial improvement in the following: 1) Improved room temperature threshold current, currently on the order of a milliampere, whereas in theory much lower threshold currents are predicted[21,23]. 2) Significant lifetimes of the devices need to be demonstrated. 3) Efficient out coupling of light or plasmons into either free space or a (plasmonic) waveguide structure will be required.

Conclusion

Recent years have seen the emergence of lasers made from small metallic structures, as well as refinements in dielectric cavity lasers and the beginning of their penetration into new areas such as biology. By considering a simple laser model, we have seen that small lasers based on dielectric and metallic cavities use different strategies to reduce the size of lasers. In general, small dielectric lasers employ cavities with long photon lifetimes to reduce demands on the laser gain medium. In contrast, metallic cavities typically have much shorter photon lifetimes, often due to absorption in the metal. Increased confinement of the optical mode to the gain medium provides a design window in which lasing can occur in the metallic structures, though the gain medium is still often pushed to its limit. Typically, dielectric small lasers have cavities with

dimensions and volumes greater than the wavelength of light, and quality factors >1,000 whereas the cavities of metal based small lasers can be smaller than the wavelength of light, and have quality factors < 1,000.

Besides providing tight confinement, the metal structures in metallic and plasmonic lasers also provide good heat-sinking and a pathway for electrical pumping, which has contributed to the rapid development of electrically pumped devices operating at room temperature. Additionally, the ever smaller lasers have stimulated useful debate in the following areas: 1) Propagation of light and gain in small lossy dispersive structures. 2) Spontaneous vs stimulated emission and the characteristics of lasers with cavity sizes well below the diffraction limit. 3) Increasing the maximum optical gain available from various gain media.

There has also been significant progress in dielectric small lasers, in particular the realization of CW electrically pumped photonic crystal lasers. These devices exhibit the lowest thresholds of all room temperature electrically pumped lasers and may thus lead to more widespread use of photonic crystal structures in photonic integrated circuits.

Another significant and exciting area of recent progress has been the application of small lasers to biology and the implementation of small lasers in biological structures themselves. Most likely, for lasers to flourish in this area, different tradeoffs will be required between the various performance and fabrication parameters than for optical communication or data processing. For instance, in diagnostics one may require large quantities of small lasers thus necessitating extremely cost-efficient fabrication but putting less stringent requirements on long-term operational stability. The maximum size of lasers applied within biological structures is imposed by nature and will vary between applications, e.g. mammalian cells measure 10-50 μm, capillary blood vessels are a few μm in diameter and the endocytic vesicles responsible for the transport of molecules and small particles across cell membranes typically have sub-μm dimensions.

Interest in making lasers smaller does not seem to have been discouraged when established laser concepts approached the conventional diffraction limit; on the contrary, recent years have clearly seen a very significant interest in making ever smaller and lower power lasers. Concrete high-impact applications where small size and low power are of key importance are starting to emerge, particularly in short distance communications. To lay the groundwork for additional applications, continued research will be necessary in small lasers, in their fundamental properties and constituent materials, and in related research areas that depend on small lasers and optical amplifiers such as plasmonics and nano-photonics.

BOX: Exciton-Polariton Lasers

According to most textbooks population inversion of the gain medium is a fundamental prerequisite for lasing. However, for many applications it is not the operation principle of the laser that is essential but rather the properties of the emitted light, i.e. coherence, directionality, monochromaticity, etc. Intense research over the past two decades has shown that exciton-polariton condensation in micro cavities represents a fundamentally different and potentially more efficient process to generate coherent light.

Exciton-polaritons are quasi-particles that form in resonators that provide strong coupling between intra-cavity photons and the excitonic states of a gain medium inside the resonator (Fig. B1a). In other words, a system is best described in the exciton-polariton picture —rather than by separately considering photons and excitons— if the rate at which photons escape from the cavity is smaller than the rate at which excitons are converted into photons and vice versa (i.e. rate of stimulated emission and absorption). In this strong coupling regime, exciton-polaritons can form a condensate or coherent state once their density becomes sufficiently high. Photon leakage from a resonator containing such a condensate yields coherent light, which is nearly indistinguishable from conventional laser emission; hence, the term exciton-polariton laser.

Strong coupling can be achieved for instance in small Fabry-Perot cavities in which the gain medium is located at the anti-nodes of the cavity photon mode (i.e. VCSEL-type structures).

Exciton-polariton condensates show unique and rich physics and their fundamental properties have been intensively studied. However, polariton lasing was initially only achieved when the condensate was repopulated by optical pumping[94,95], similar to the initial situation with plasmon mode metallic lasers. Very recently, electrically pumped polariton lasing has also been demonstrated, even though only at cryogenic temperatures and substantial magnetic fields (Fig. B1b and c)[96,97].

The device structure of a polariton laser can be analogous to a conventional VCSEL and polariton lasers will show conventional photonic lasing if excited above population inversion. In fact, the presence of two distinct thresholds, the lower associated with polariton lasing and the higher associated with conventional photon lasing, is regarded as a sign of polariton condensation (Fig. B1c)[98]. As polariton condensation does not require inversion, future polariton lasers may operate at considerably lower pump powers than photonic lasers.

Polariton condensation is an ensemble effect requiring the presence of multiple polaritons and therefore shows a clear threshold behavior. Although this threshold can be very small, one does not expect quasi threshold-less lasing, as found for conventional lasing in resonators with large spontaneous emission factors (β-factors, compare Fig. 4b).

Most work on polariton lasers is based on GaN or GaAs based cavities. However, organic materials are also interesting candidates for polariton devices, in particular due to their low residual absorption and their short-lived, highly localized excited states. Organic-loaded VCSEL structures have recently shown room-temperature polariton lasing and polariton condensation[99,100].

Author contributions

Both authors contributed equally to this article

Additional information

Correspondence and requests for materials can be addressed to either M.C.G. or M.T.H.

Competing financial interests

The authors declare no competing financial interests.

Acknowledgements

M.T.H was supported by an Australian Research council Future Fellowship research grant for this work. M.C.G. is grateful to the Scottish Funding Council (via SUPA) for financial support.

References

1. Miller, D. A. B. Device Requirements for Optical Interconnects to Silicon Chips. *Proc. IEEE* **97,** 1166–1185 (2009).
2. Smit, M. K., van der Tol, J. & Hill, M. T. Moore's law in photonics. *Laser Photon. Rev.* **6,** 1–13 (2012).
3. Leuthold, J. *et al.* Plasmonic Communications: Light on a Wire. *Opt. Photonics News* **24,** 28–35 (2013).
4. Gather, M. C. & Yun, S. H. Single-cell biological lasers. *Nat. Photonics* **5,** 406–410 (2011).
5. Kim, T. *et al.* Injectable, cellular-scale optoelectronics with applications for wireless optogenetics. *Science* **340,** 211–216 (2013).
6. Blanche, P.-A. *et al.* Holographic three-dimensional telepresence using large-area photorefractive polymer. *Nature* **468,** 80–83 (2010).
7. Iga, K. Surface-emitting laser - its birth and generation of new optoelectronics field. *IEEE J. Sel. Top. Quantum Electron.* **6,** 1201–1215 (2000).
8. Lee, Y. H. *et al.* Room-temperature cw vertical cavity single quantum well microlaser diodes. *Electron. Lett.* **25,** 1377–1378 (1989).
9. Levi, A. F. J. *et al.* Room temperature operation of microdisc lasers with submilliamp threshold current. *Electron. Lett.* **28,** 1010–1012 (1992).
10. Painter, O. *et al.* Two-Dimensional Photonic Band-Gap Defect Mode Laser. *Science* **284,** 1819–1821 (2010).
11. Huang, M. H. *et al.* Room-temperature ultraviolet nanowire nanolasers. *Science* **292,** 1897–1899 (2001).
12. Samuel, I. D. W. & Turnbull, G. A. Organic semiconductor lasers. *Chem. Rev.* **107,** 1272–1295 (2007).
13. Klimov, V. I. *et al.* Optical Gain and Stimulated Emission in Nanocrystal Quantum Dots. *Science* **290,** 314–317 (2000).
14. Gramotnev, D. K. & Bozhevolnyi, S. I. Plasmonics beyond the diffraction limit. *Nat. Photonics* **4,** 83–91 (2010).
15. Barnes, W. L., Dereux, A. & Ebbesen, T. W. Surface plasmon subwavelength optics. *Nature* **424,** 824–830 (2003).
16. Zia, R., Selker, M. D., Catrysse, P. B. & Brongersma, M. L. Geometries and materials for subwavelength surface plasmon modes. *J. Opt. Soc. Am. A. Opt. Image Sci. Vis.* **21,** 2442–2446 (2004).
17. Hill, M. T. *et al.* Lasing in metallic-coated nanocavities. *Nat. Photonics* **1,** 589–594 (2007).
18. Hill, M. T. *et al.* Lasing in metal-insulator-metal sub-wavelength plasmonic waveguides. *Opt. Express* **17,** 11107–11112 (2009).
19. Noginov, M. A. *et al.* Demonstration of a spaser-based nanolaser. *Nature* **460,** 1110–1112 (2009).
20. Oulton, R. F. *et al.* Plasmon lasers at deep subwavelength scale. *Nature* **461,** 629–632 (2009).
21. Chang, S.-W., Lin, T.-R. & Chuang, S. L. Theory of plasmonic fabry-perot nanolasers. *Opt. Express* **18,** 15039–15053 (2010).
22. Ning, C.-Z. Semiconductor Nanolasers. *Phys. Status Solidi B* **247,** 774–788 (2010).
23. Ni, C.-Y. A. & Chuang, S. L. Theory of high-speed nanolasers and nanoLEDs. *Opt. Express* **20,** 16450 (2012).
24. Li, D. & Stockman, M. I. Electric Spaser in the extreme quantum limit. *Phys. Rev. Lett.* **110,** 106803 (2013).
25. Ma, R.-M., Oulton, R. F., Sorger, V. J. & Zhang, X. Plasmon lasers: coherent light source at molecular scales. *Laser Photon. Rev.* **7,** 1–21 (2013).
26. Chuang, S. L. *Physics of Photonic Devices, 2nd Ed.* (John Wiley & Sons, New Jersey, 2009).
27. Hill, M. T. Metal-Insulator-Metal Waveguides With Self Aligned and Electrically Contacted Thin Semiconductor Cores Exhibiting High Optical Confinement and Low Loss. *J. Light. Technol.* **31,** 2540–2549 (2013).
28. Kirstaedter, N. *et al.* Gain and differential gain of single layer InAs/GaAs quantum dot injection lasers. *Appl. Phys. Lett.* **69,** 1226 (1996).
29. Chen, R. *et al.* Nanolasers grown on silicon. *Nat. Photonics* **5,** 170–175 (2011).
30. Saxena, D. *et al.* Optically pumped room-temperature GaAs nanowire lasers. *Nat. Photonics* **7,** 963–968 (2013).
31. Ding, K. *et al.* Record performance of electrical injection sub-wavelength metallic-cavity semiconductor lasers at room temperature. *Opt. Express* **21,** 4728–4733 (2013).
32. Lu, C.-Y., Chang, S.-W., Chuang, S. L., Germann, T. D. & Bimberg, D. Metal-cavity surface-emitting microlaser at room temperature. *Appl. Phys. Lett.* **96,** 251101 (2010).
33. O'Carroll, D., Lieberwirth, I. & Redmond, G. Microcavity effects and optically pumped lasing in single conjugated polymer nanowires. *Nat. Nanotechnol.* **2,** 180–184 (2007).

34. Nishijima, Y. *et al.* Lasing with well-defined cavity modes in dye-infiltrated silica inverse opals. *Opt. Express* **17,** 2976–2983 (2009).
35. Mizuno, H. *et al.* Single Crystals of 5,5′-Bis(4′-methoxybiphenyl-4-yl)-2,2′-bithiophene for Organic Laser Media. *Adv. Mater.* **24,** 5744–5749 (2012).
36. Riechel, S. *et al.* Very compact tunable solid-state laser utilizing a thin-film organic semiconductor. *Opt. Lett.* **26,** 593–595 (2001).
37. Shapira, O. *et al.* Surface-emitting fiber lasers. *Opt. Express* **14,** 3929–3935 (2006).
38. Tang, S. K. Y. *et al.* A multi-color fast-switching microfluidic droplet dye laser. *Lab Chip* **9,** 2767–2771 (2009).
39. Song, W., Vasdekis, A. E., Li, Z. & Psaltis, D. Optofluidic evanescent dye laser based on a distributed feedback circular grating. *Appl. Phys. Lett.* **94,** 161110 (2009).
40. Kuehne, A. J. C. *et al.* A switchable digital microfluidic droplet dye-laser. *Lab Chip* **11,** 3716–3719 (2011).
41. Ubukata, T., Isoshima, T. & Hara, M. Wavelength-Programmable Organic Distributed-Feedback Laser Based on a Photoassisted Polymer-Migration System. *Adv. Mater.* **17,** 1630–1633 (2005).
42. Kuwata-Gonokami, M., Takeda, K., Yasuda, H. & Ema, K. Laser Emission from Dye-Doped Polystyrene Microsphere. *Jpn. J. Appl. Phys.* **31,** L99–L101 (1992).
43. Yap, B. K., Xia, R., Campoy-Quiles, M., Stavrinou, P. N. & Bradley, D. D. C. Simultaneous optimization of charge-carrier mobility and optical gain in semiconducting polymer films. *Nat. Mater.* **7,** 376–380 (2008).
44. Wang, H. *et al.* Cyano-Substituted Oligo(p-phenylene vinylene) Single Crystals: A Promising Laser Material. *Adv. Funct. Mater.* **21,** 3770–3777 (2011).
45. Tsiminis, G. *et al.* Nanoimprinted organic semiconductor laser pumped by a light-emitting diode. *Adv. Mater.* **25,** 2826–2830 (2013).
46. Anikeeva, P. O., Halpert, J. E., Bawendi, M. G. & Bulovic, V. Quantum Dot Light-Emitting Devices with Electroluminescence Tunable over the Entire Visible Spectrum. *Nano Lett.* **9,** 2532–2536 (2009).
47. Dang, C. *et al.* Red, green and blue lasing enabled by single-exciton gain in colloidal quantum dot films. *Nat. Nanotechnol.* **7,** 335–339 (2012).
48. Lebby, M. S. *et al.* Use of VCSEL arrays for parallel optical interconnects. in *Proc. SPIE Fabr. Testing, Reliab. Semicond. Lasers 2683* 81–91 (1996).
49. Yang, G. M., MacDougal, M. H. & Dapkus, P. D. Ultralow threshold current vertical-cavity surface-emitting lasers obtained with selective oxidation. *Electron. Lett.* **31,** 886–888 (1995).
50. Langner, M., Sudzius, M., Fröb, H., Lyssenko, V. G. & Leo, K. Selective excitation of laser modes in an organic photonic dot microcavity. *Appl. Phys. Lett.* **95,** 091109 (2009).
51. Gather, M. C. & Yun, S. H. Lasing from Escherichia coli bacteria genetically programmed to express green fluorescent protein. *Opt. Lett.* **36,** 3299–3301 (2011).
52. Polman, A., Min, B., Kalkman, J., Kippenberg, T. J. & Vahala, K. J. Ultralow-threshold erbium-implanted toroidal microlaser on silicon. *Appl. Phys. Lett.* **84,** 1037 (2004).
53. Fujita, M., Ushigome, R. & Baba, T. Continuous wave lasing in GaInAsP microdisk injection laser with threshold current of 40 μA. *Electron. Lett.* **36,** 790–791 (2000).
54. Zhang, Z. *et al.* Visible submicron microdisk lasers. *Appl. Phys. Lett.* **90,** 111119 (2007).
55. Van Campenhout, J. *et al.* Low-Footprint Optical Interconnect on an SOI Chip Through Heterogeneous Integration of InP-Based Microdisk Lasers and Microdetectors. *IEEE Photonics Technol. Lett.* **21,** 522–524 (2009).
56. Spillane, S. M., Kippenberg, T. J. & Vahala, K. J. Ultralow-threshold Raman laser using a spherical dielectric microcavity. *Nature* **415,** 621–623 (2002).
57. Park, H.-G. *et al.* Electrically driven single-cell photonic crystal laser. *Science* **305,** 1444–1447 (2004).
58. Tandaechanurat, A. *et al.* Lasing oscillation in a three-dimensional photonic crystal nanocavity with a complete bandgap. *Nat. Photonics* **5,** 91–94 (2011).
59. Takeda, K., Sato, T., Shinya, A. & Nozaki, K. Few-fJ/bit data transmissions using directly modulated lambda-scale embedded active region photonic-crystal lasers. *Nat. Photonics* **7,** 569–575 (2013).
60. Karnutsch, C. *et al.* Improved organic semiconductor lasers based on a mixed-order distributed feedback resonator design. *Appl. Phys. Lett.* **90,** 131104 (2007).

61. Kuehne, A. J. C. *et al.* Sub-Micrometer Patterning of Amorphous- and β-Phase in a Crosslinkable Poly(9,9-dioctylfluorene): Dual-Wavelength Lasing from a Mixed-Morphology Device. *Adv. Funct. Mater.* **21,** 2564–2570 (2011).
62. Baumann, K. *et al.* Organic mixed-order photonic crystal lasers with ultrasmall footprint. *Appl. Phys. Lett.* **91,** 171108 (2007).
63. Nezhad, M. P. *et al.* Room-temperature subwavelength metallo-dielectric lasers. *Nat. Photonics* **4,** 395–399 (2010).
64. Yu, K., Lakhani, A. & Wu, M. C. Subwavelength metal-optic semiconductor nanopatch lasers. *Opt. Express* **18,** 8790–8799 (2010).
65. Lu, C.-Y. *et al.* Low Thermal Impedance of Substrate-Free Metal Cavity Surface-Emitting Microlasers. *IEEE Photonics Technol. Lett.* **23,** 1031–1033 (2011).
66. Fukui, M., So, V. C. Y. & Normandin, R. Lifetime of Surface Plasmons in Thin Silver Films. *Phys. Status Solidi B* **91,** K61–K64 (1979).
67. Gather, M. C., Meerholz, K., Danz, N. & Leosson, K. Net optical gain in a plasmonic waveguide embedded in a fluorescent polymer. *Nat. Photonics* **4,** 457–461 (2010).
68. De Leon, I. & Berini, P. Amplification of long-range surface plasmons by a dipolar gain medium. *Nat. Photonics* **4,** 382–387 (2010).
69. Lakhani, A. M., Kim, M., Lau, E. K. & Wu, M. C. Plasmonic crystal defect nanolaser. *Opt. Express* **19,** 18237–18245 (2011).
70. Perahia, R., Alegre, T. P. M., Safavi-Naeini, A. H. & Painter, O. Surface-plasmon mode hybridization in subwavelength microdisk lasers. *Appl. Phys. Lett.* **95,** 201114 (2009).
71. Kwon, S.-H. *et al.* Subwavelength plasmonic lasing from a semiconductor nanodisk with silver nanopan cavity. *Nano Lett.* **10,** 3679–83 (2010).
72. Lu, Y.-J. *et al.* Plasmonic nanolaser using epitaxially grown silver film. *Science* **337,** 450–453 (2012).
73. Leosson, K. *et al.* Ultra-thin gold films on transparent polymers. *Nanophotonics* **2,** 3–11 (2013).
74. Ma, R.-M., Oulton, R. F., Sorger, V. J., Bartal, G. & Zhang, X. Room-temperature sub-diffraction-limited plasmon laser by total internal reflection. *Nat. Mater.* **10,** 110–113 (2011).
75. Khajavikhan, M. *et al.* Thresholdless nanoscale coaxial lasers. *Nature* **482,** 204–207 (2012).
76. Bergman, D. J. & Stockman, M. I. Surface plasmon amplification by stimulated emission of radiation: quantum generation of coherent surface plasmons in nanosystems. *Phys. Rev. Lett.* **90,** 027402 (2003).
77. Meng, X., Kildishev, A. V, Fujita, K., Tanaka, K. & Shalaev, V. M. Wavelength-tunable spasing in the visible. *Nano Lett.* **13,** 4106–4112 (2013).
78. Peng, B. *et al.* Fluorophore-doped core-multishell spherical plasmonic nanocavities: resonant energy transfer toward a loss compensation. *ACS Nano* **6,** 6250–6259 (2012).
79. Li, X. F. & Yu, S. F. Design of low-threshold compact Au-nanoparticle lasers. *Opt. Lett.* **35,** 2535–2537 (2010).
80. Khurgin, J. B. & Sun, G. Injection pumped single mode surface plasmon generators: threshold, linewidth, and coherence. *Opt. Express* **20,** 15309 (2012).
81. Suh, J. Y. *et al.* Plasmonic Bowtie Nanolaser Arrays. *Nano Lett.* **12,** 5769–5774 (2012).
82. Zhou, W. *et al.* Lasing action in strongly coupled plasmonic nanocavity arrays. *Nat. Nanotechnol.* **8,** 506–511 (2013).
83. Meng, X., Fujita, K., Murai, S., Matoba, T. & Tanaka, K. Plasmonically controlled lasing resonance with metallic-dielectric core-shell nanoparticles. *Nano Lett.* **11,** 1374–1378 (2011).
84. Kim, M.-K., Lakhani, A. M. & Wu, M. C. Efficient waveguide-coupling of metal-clad nanolaser cavities. *Opt. Express* **19,** 23504–23512 (2011).
85. Ma, R.-M., Yin, X., Oulton, R. F., Sorger, V. J. & Zhang, X. Multiplexed and electrically modulated plasmon laser circuit. *Nano Lett.* **12,** 5396–5402 (2012).
86. He, L., Özdemir, S. K., Zhu, J., Kim, W. & Yang, L. Detecting single viruses and nanoparticles using whispering gallery microlasers. *Nat. Nanotechnol.* **6,** 428–432 (2011).
87. Francois, A. & Himmelhaus, M. Whispering gallery mode biosensor operated in the stimulated. *Appl. Phys. Lett.* **94,** 031101 (2009).
88. Nizamoglu, S., Gather, M. C. & Yun, S. H. All-Biomaterial Laser using Vitamin and Biopolymers. *Adv. Mater.* **25,** 5943–5947 (2013).

89. Sun, Y., Shopova, S. I., Wu, C., Arnold, S. & Fan, X. Bioinspired optofluidic FRET lasers via DNA scaffolds. *Proc. Natl. Acad. Sci. U. S. A.* **107,** 16039–16042 (2010).
90. Long, C. M., Giannopoulos, A. V. & Choquette, K. D. Modified spontaneous emission from laterally injected photonic crystal emitter. *Electron. Lett.* **45,** 227–228 (2009).
91. Shambat, G. *et al.* Electrically Driven Photonic Crystal Nanocavity Devices. *IEEE J. Sel. Top. Quantum Electron.* **18,** 1700–1710 (2012).
92. Symonds, C. *et al.* Confined Tamm Plasmon Lasers. *Nano Lett.* **13,** 3179–3184 (2013).
93. Van Beijnum, F. *et al.* Surface Plasmon Lasing Observed in Metal Hole Arrays. *Phys. Rev. Lett.* **110,** 206802 (2013).
94. Kasprzak, J. *et al.* Bose-Einstein condensation of exciton polaritons. *Nature* **443,** 409–414 (2006).
95. Christopoulos, S. *et al.* Room-temperature polariton lasing in semiconductor microcavities. *Phys. Rev. Lett.* **98,** 126405 (2007).
96. Schneider, C. *et al.* An electrically pumped polariton laser. *Nature* **497,** 348–352 (2013).
97. Bhattacharya, P., Xiao, B., Das, A., Bhowmick, S. & Heo, J. Solid State Electrically Injected Exciton-Polariton Laser. *Phys. Rev. Lett.* **110,** 206403 (2013).
98. Tempel, J.-S. *et al.* Characterization of two-threshold behavior of the emission from a GaAs microcavity. *Phys. Rev. B* **85,** 075318 (2012).
99. Kéna-Cohen, S. & Forrest, S. R. Room-temperature polariton lasing in an organic single-crystal microcavity. *Nat. Photonics* **4,** 371–375 (2010).
100. Klaers, J., Schmitt, J., Vewinger, F. & Weitz, M. Bose-Einstein condensation of photons in an optical microcavity. *Nature* **468,** 545–548 (2010).
101. Kwon, S. H., Park, H. G. & Lee, Y. H. Photonic Crystal Lasers. *Semicond. Semimetals* **86,** 301–333 (2012).
102. Baba, T., Fujita, M. & Sakai, A. Lasing characteristics of GaInAsP-InP strained qunatum-well microdisk injection lasers with diameter of 2-10 µm. *IEEE Photonics Technol. Lett.* **9,** 878–880 (1997).
103. Seo, M.-K. *et al.* Low threshold current single-cell hexapole mode photonic crystal laser. *Appl. Phys. Lett.* **90,** 171122 (2007).

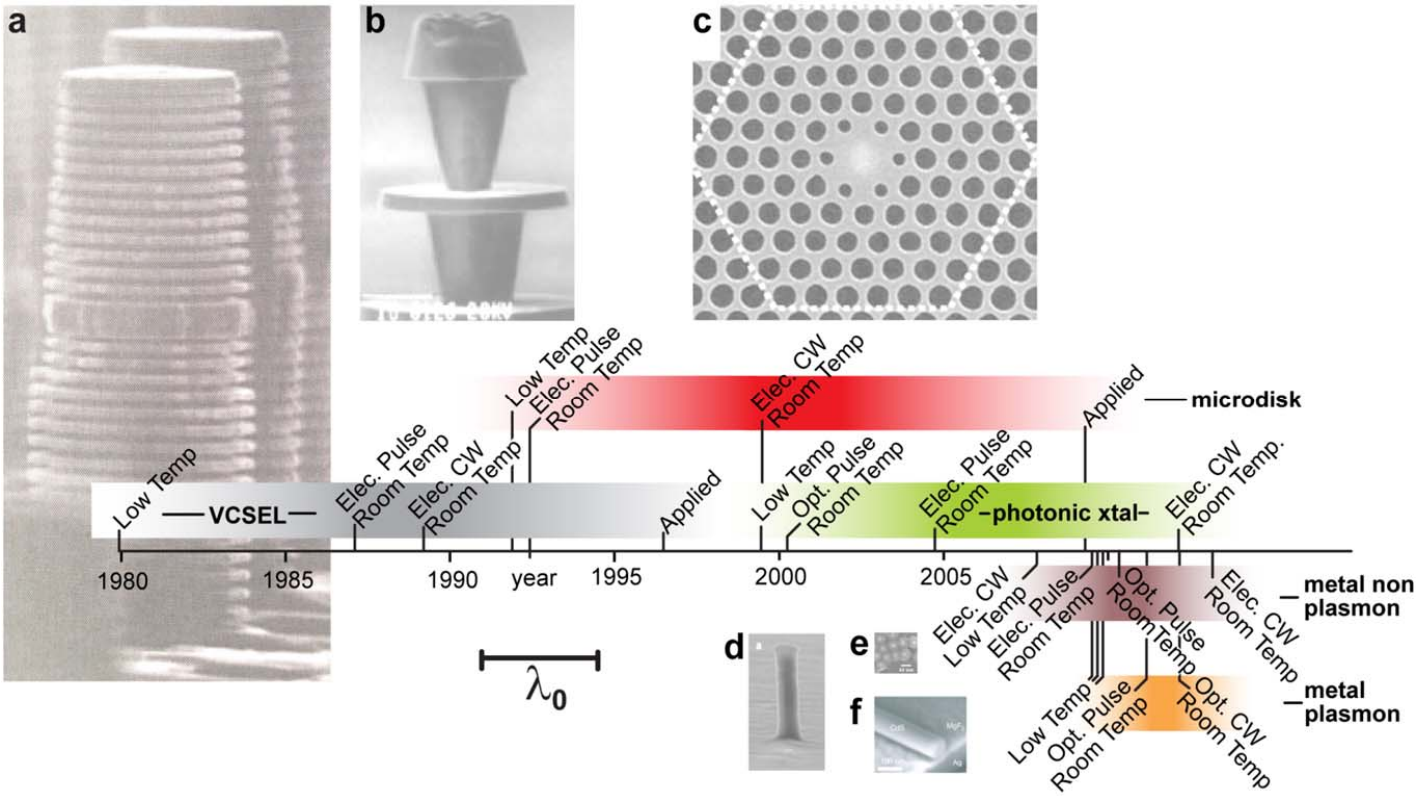

Figure 1. Timeline of the development of various forms of small lasers from first demonstration to electrical, CW and room temperature operation, and in some cases already to commercial applications. The development time from initial demonstrations of a new laser concept to applications is 10 to 20 years. However, compared to conventional dielectric small lasers, recently developed metal cavity lasers have seen a very rapid development. (CW – continuous operation.) Also shown is a size comparison of various types of small laser (adapted from Ref. [101]). The electron microscopy pictures are scaled to the free space emission wavelength λ_0 of each laser. **a**, VCSEL (from Ref. [101]), **b**, microdisk laser (from Ref. [102]), **c**, photonic crystal laser (from Ref. [103]), **d**, metallic non-plasmon mode laser (from Ref. [17]), **e**, localized plasmon mode laser (from Ref. [19]), **f**, metallic propagating plasmon mode laser (from Ref. [20]). The metal cavity lasers developed recently exhibit a dramatic reduction in size compared to dielectric cavity lasers. (See Supplementary Information Fig. S1 for references to data points on the timeline.)

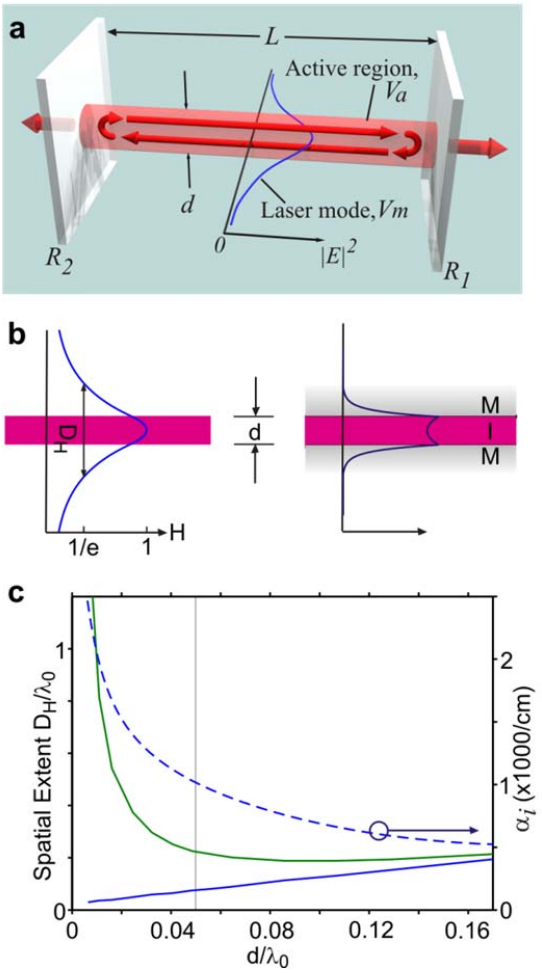

Figure 2. Fundamental challenges involved in laser miniaturization, illustrated considering a simple Fabry-Perot resonator laser. a, Schematic of Fabry-Perot resonator. The minimum length *L* of the laser resonator is given by a phase matching limit and a gain limit (i.e. light extraction losses at the two mirrors – with reflectivity R_1 and R_2 – and internal absorption losses α_i have to be compensated). The minimum volume of the active region V_a is also determined by the gain limit. **b**, The total mode volume V_m determined by the mode electric field profile $|E|^2$, depends on the geometry of the resonator and the transverse dimensions of the Fabry-Perot laser and can be reduced by tuning the diameter *d* of the active material waveguide between the mirrors. For a thin dielectric waveguide (left), the spatial extent D_H of the transverse *H* field is greater than for the plasmon gap mode of a metal-insulator-metal (MIM) waveguide (right). **c**, D_H*versus d* with both normalized to the free space emission wavelength λ_0, for dielectric (green line) and MIM (blue line) waveguides. The reduced D_H of the MIM waveguide comes at the cost of increased α_i (dashed blue line). Calculations assume λ_0 = 1.55μm, silver as metal, 3.6 as bulk refractive index for the active material and surrounding dielectric is air. The grey vertical line indicates the example values given in the text.

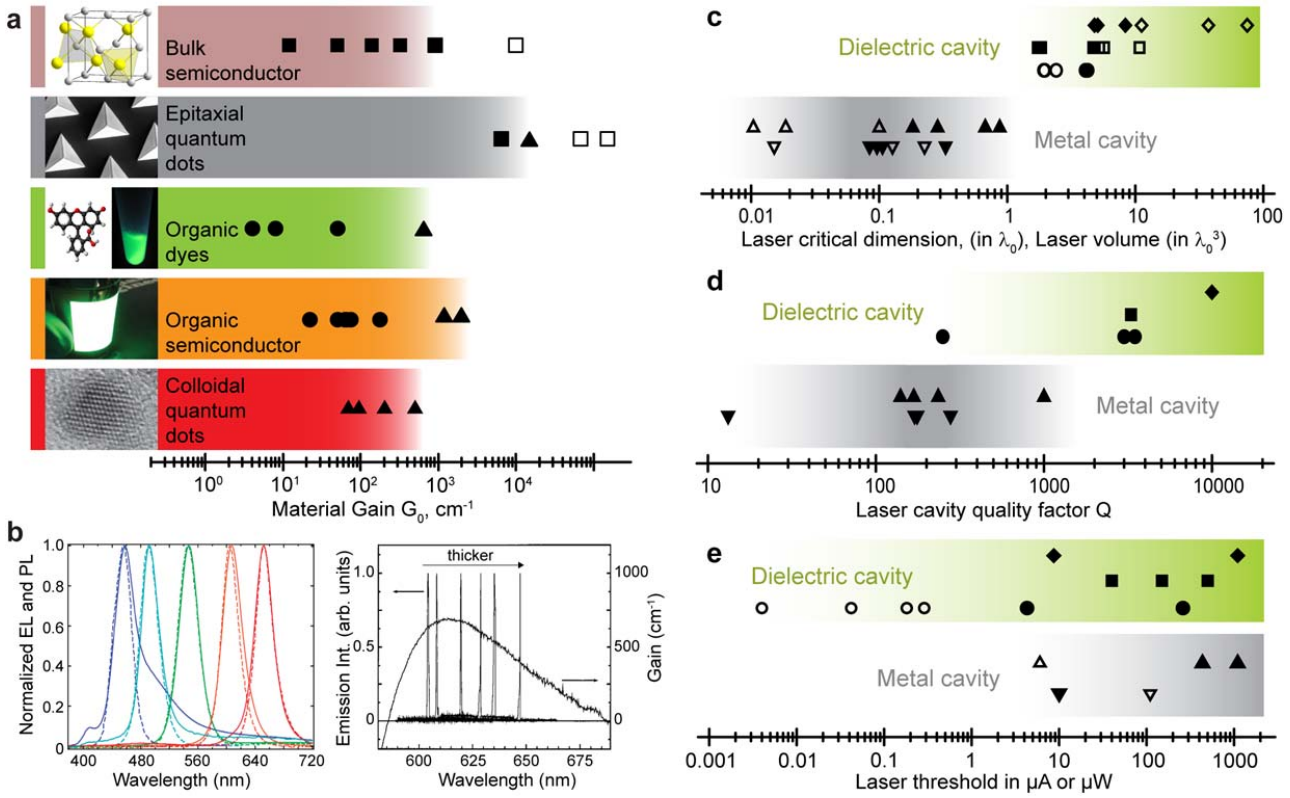

Figure 3. Overview of optical gain materials considered for use in small lasers and key properties of various small lasers. **a**, Typical net material gain G_0 available from different classes of materials. Color bars give approximate indication of the gain achievable in practice. Points represent values reported in the literature: squares – electrical pumping, circles – ASE data with ns optical pumping, triangles – data for sub-ps optical excitation, open symbols – Gain achieved at cryogenic temperatures. (See Supplementary Information Fig. S2 for references to each data point and to the illustrative pictures.) **b**, Emission and gain spectra of colloidal quantum dots, organic dyes, and organic semiconductors are broad and can be tuned by chemical modification or size variation. Photoluminescence and electroluminescence spectra from five different types of colloidal quantum dots, spanning the entire visible spectrum (left, Ref. [46]). Tuning the emission wavelength of organic semiconductor based DFB lasers by adjusting gain layer thickness (right, Ref. [36]). **c**, Minimum extent of small lasers in one dimension (solid symbols) and minimum volume (open symbols), both relative to the free space wavelength λ_0 of the emitted light. For the same lasers, **d**, *Q* factor and **e**, threshold in μW (CW optical pumping) and in μA (electrical pumping, pulsed or CW). Open symbols: cryogenic temperatures. Filled symbols: RT. On green bars: diamonds – VCSELs, squares - microdisk, circles – photonic crystal; on grey bars: triangles up – metallic non-plasmon mode, triangles down – metallic plasmon mode. Note the clear divide in size and *Q* factor between the dielectric and metal cavity lasers. Photonic crystal lasers with few quantum dot gain medium show exceptionally low threshold currents at low temperatures. (See Supplementary Information Fig. S3 for references to each data point.)

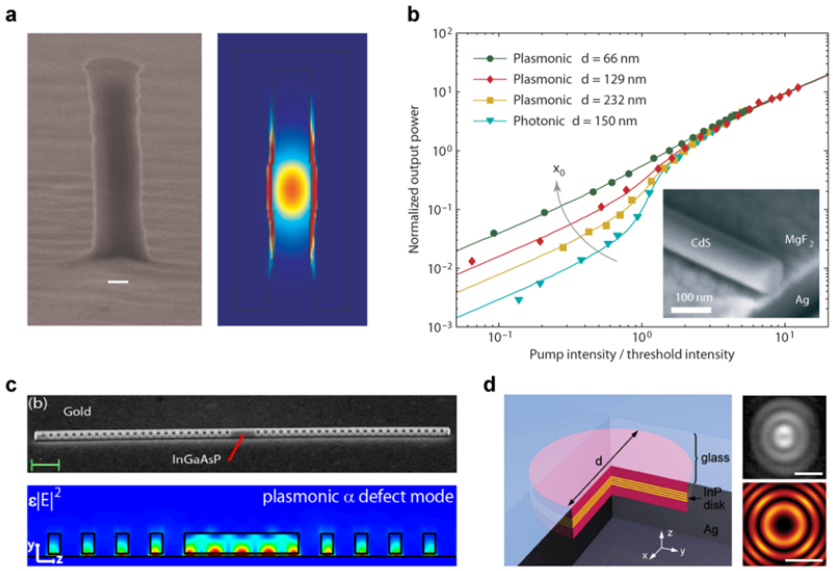

Figure 4. Metal based lasers. a, Gold embedded nano-pillar laser operating on a HE (hybrid electric) mode. Scanning electron microscopy (SEM) image of a fabricated pillar, without the surrounding gold (left, scale bar 103 nm) and simulation of electric-field intensity of the optical mode in the fabricated pillar (right). (Reproduced from Ref. [17]) **b**, Input-output characteristics of a hybrid plasmonic waveguide laser consisting of a high-gain cadmium-sulfide nanowire, separated from a silver surface by a 5-nm thick insulating gap. A photonic laser with a nanowire on a quartz substrate is also shown. For low nanowire diameters *d*, the plasmonic device shows quasi thresholdless lasing. Inset: SEM image of structure. (Reproduced from Ref. [20]) **c**, Plasmonic crystal nanolaser based on a linear semiconductor defect structure on a gold surface. SEM image (top) and optical simulation of the electric energy density of the plasmonic mode (bottom). (Reproduced from Ref. [69]) **d**, Whispering-gallery mode plasmonic nano-disk based on a semiconductor quantum well structure embedded in silver. Structure of device (left), experimentally observed unpolarized emission for cavity with d = 1 µm (top right) and corresponding optical simulation (bottom right); scale bars 2 µm. (Reproduced from Ref. [71])

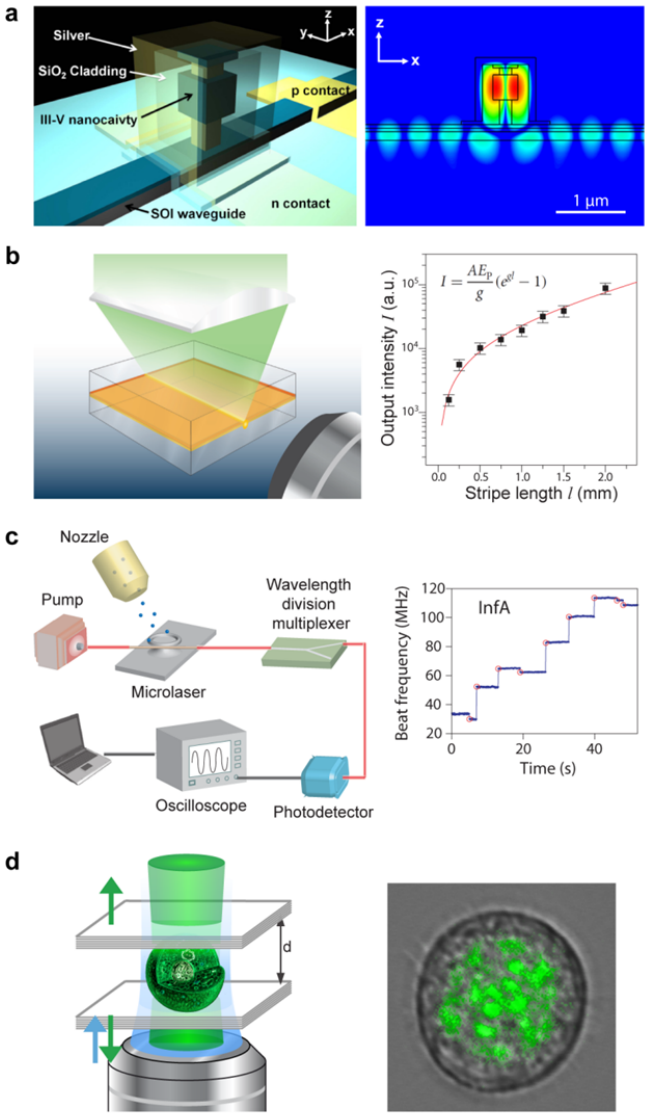

Figure 5. Envisaged future applications of small lasers. a, On-chip and short distance optical communication with small lasers requires compact coupling schemes. Schematic of a proposed metal-clad laser coupled to a SOI-waveguide (left) and finite-difference time-domain simulation of the coupling from laser cavity in the center to the waveguide beneath (right). (Reproduced from Ref. [84]) **b**, Energy can also be coupled to a plasmonic waveguide, but the large losses in these waveguides may require active loss compensation. Schematic of slab plasmon waveguide amplifier with ultra-thin gold film between optically pumped organic semiconductor layers (left). Output intensity *I* from waveguide edge grows exponentially with the length *l* of the pumped segment, indicating amplified spontaneous emission and net optical gain. Inset: the gain equation with gain coefficient *g* and proportionality constant AE_P (right). (Reproduced from Ref. [67]) **c**, Small lasers are also useful for ultra-sensitive detection, e.g. using a fibre coupled whispering gallery microlaser (left). Binding of individual influenza A (InfA) virus particles leads to mode splitting and to a beat frequency related to the number of bound particles (right). (Reproduced from Ref. [86]) **d**, A single biological cell can form a small laser if genetically programmed to produce green fluorescent protein (GFP). Schematic of a first single cell laser (left) and typical spatial emission pattern (right). (Reproduced from Ref. [4])

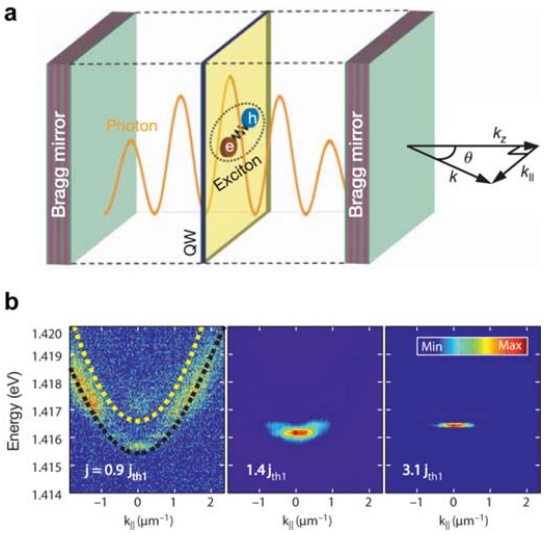

Figure B1. Exciton-polariton lasers. a, Illustration of VCSEL structure used to study exciton-polariton condensation. The planar Bragg mirrors enclosing a quantum well (QW) based gain medium quantize the longitudinal wave vector (k_z) without restricting the in-plane wave vector ($k_{||}$). (Reproduced from Ref. [94]). **b**, Momentum and energy resolved emission from an electrically pumped exciton-polariton laser under a magnetic field of 5 T; below condensation threshold, around threshold current (j_{th1}) and well above threshold. (Reproduced from Ref. [96])